# Comparison and Evaluation of Feature Point Detectors

**VOLKER RODEHORST**
Computer Vision & Remote Sensing
Berlin University of Technology, Germany

**ANDREAS KOSCHAN**
Imaging, Robotics and Intelligent Systems
The University of Tennessee, Knoxville, USA

5th International Symposium
„Turkish-German Joint Geodetic Days“
March 29-31, 2006
Berlin

# Feature-based Image Matching

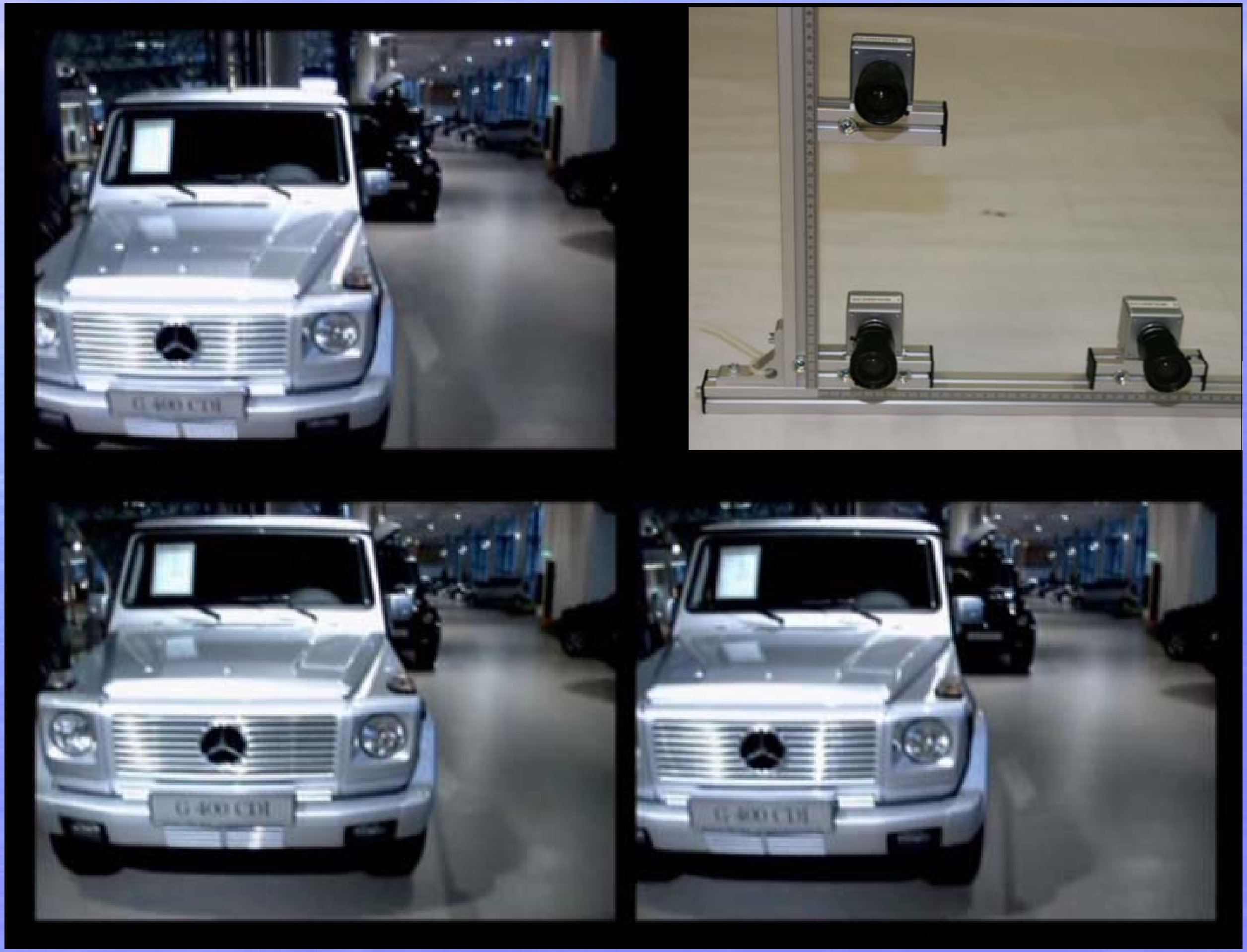

# Egomotion Estimation

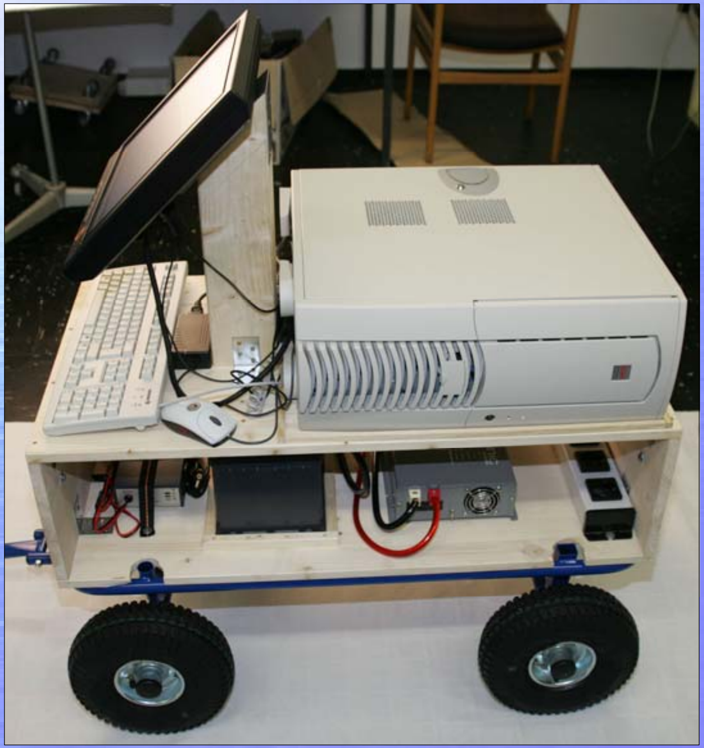

# Overview

- **Introduction**
  - Interest Operators (Plessey, Förstner, SUSAN-2D)
- **Improvements and Extensions**
  - Sub-pixel Localization
  - Extension for Color Images
  - Uniform Point Distribution
- **Comparison and Evaluation**
  - Detection Rate
  - Repeatability Rate
  - Localization Accuracy
- **Conclusions and Outlook**

# Requirements

- **Optimal Interest Operator** (Haralick & Shapiro, 1992):
  - Local **Distinctness**
  - **Invariance** against distortions
  - **Stability** to noise and blunders
  - Global **Uniqueness**
  - **Interpretability** due to a significant meaning

# State-of-the-Art

- A Selection of Feature Point Detectors:
  - First Interest Operator (**Moravec**, 1977)
  - **Förstner** Operator (Förstner, 1987/94)
  - **Plessey** Point Detector (Harris & Stephens, 1988)
  - **SUSAN-2D** Operator (Smith & Brady, 1997)
  - Improved **Structure Tensor** (Köthe, 2003)
  - Affine Invariant **Plessey-Laplacian** (Mikolajczyk & Schmid, 2004)
  - Scale Invariant Feature Transform **SIFT** (Lowe, 2004)

# Related Work

- **Practical Comparison** (Schmid et al., 2000)
  (Förstner, Plessey, Cottier, Heitger and Horaud)
- **Definition of Saliency** (Hall et al., 2002)
  (Plessey, Plessey-Laplacian, Lindeberg)
- **Bayesian Estimation** (Sojka, 2003)
  (Plessey, SUSAN-2D, Deriche-Giraudon, Beaudet, Noble and Kitchen-Rosenfeld)
- **Synthetic Comparison** (Johansson et al. 2004)
  (Plessey, Star-Pattern-Method, 4th-Order-Tensor)
- **Mathematical Comparison** (Zuliani, 2004)
  (Plessey, Noble, Kanade-Lucas-Tomasi and Kenney)

# Continuous Differential Operators

$$f_x(x,y) = \frac{\partial}{\partial x}\left(G(x,y,\sigma) * f(x,y)\right) = \frac{\partial G(x,y,\sigma)}{\partial x} * f(x,y)$$

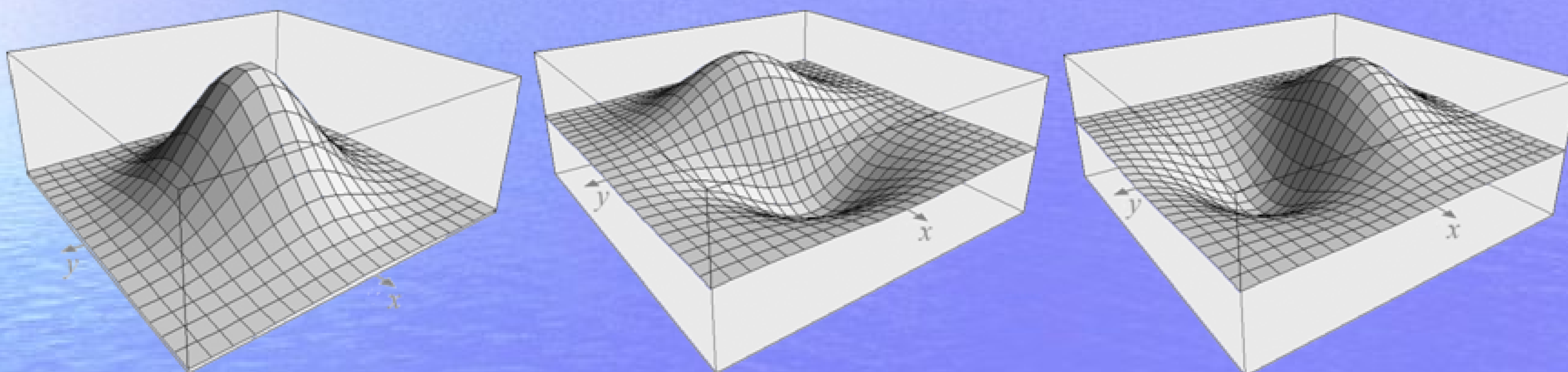


- Implementation Details
  - The filter is steered only by the **standard deviation** $\sigma$
  - The **filter size** can automatically be estimated
  - The 2D-Operator is separated in two **linear filters**

# Plessey Point Detector

- Autocorrelation Matrix:

$$\mathbf{A}(x,y)=\begin{bmatrix}\sum\limits_{i,j\in\Omega} f_x(i,j)^2 & \sum\limits_{i,j\in\Omega} f_x(i,j)\cdot f_y(i,j)\\ \sum\limits_{i,j\in\Omega} f_x(i,j)\cdot f_y(i,j) & \sum\limits_{i,j\in\Omega} f_y(i,j)^2\end{bmatrix}$$

- Characteristics of $\mathrm{A}$
  - **Rank 2**: A full rank indicates a **salient point**
  - **Rank 1**: A singular matrix suggests a **straight edge**
  - **Rank 0**: The matrix defines a **homogeneous area**
- Corner Response Function

$$w=\det(\mathbf{A})-k\cdot\mathrm{trace}(\mathbf{A})^2 \qquad k=0.05$$

# Förstner Operator

- Structure tensor:

$$\mathbf{A} = G_{\sigma_2} * \begin{bmatrix} f_x^{\,2} & f_x \cdot f_y \\ f_x \cdot f_y & f_y^{\,2} \end{bmatrix}$$

- Eigenvalues of $\mathrm{A}^{-1}$ define error ellipses:

$$w = \frac{\lambda_1 \cdot \lambda_2}{\lambda_1 + \lambda_2} = \frac{\det(\mathbf{A})}{\operatorname{trace}(\mathbf{A})} \qquad q = 1 - \left(\frac{\lambda_1 - \lambda_2}{\lambda_1 + \lambda_2}\right)^2 = \frac{4 \cdot \det(\mathbf{A})}{\operatorname{trace}(\mathbf{A})^2}$$

- Properties:
  - **Small** circular ellipses define a **salient point**
  - **Elongated** error ellipses suggest a **straight edge**
  - **Large** ellipses mark a **homogeneous area**

# Intermediate Results

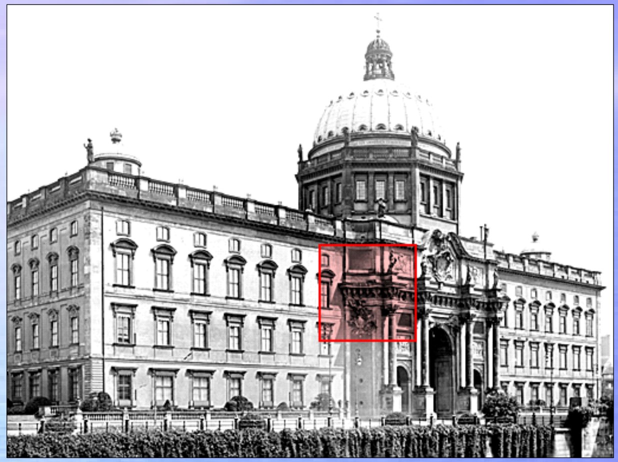
Image of Berlin Palace

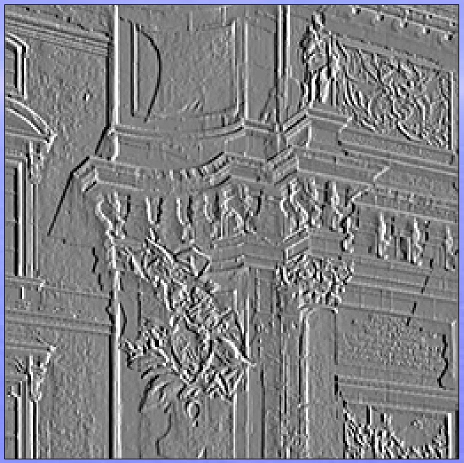
Horizontal derivative

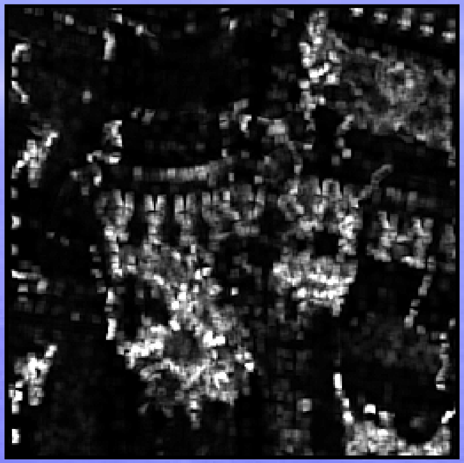
Error ellipse size


Facade section

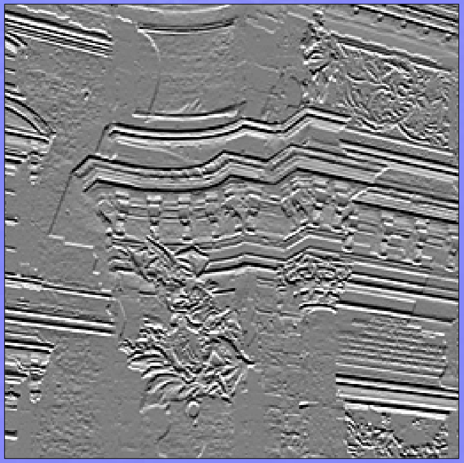
Vertical derivative

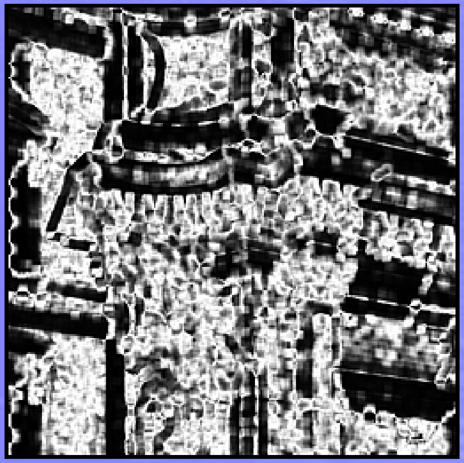
Ellipse form factor

# Sub-Pixel Extension

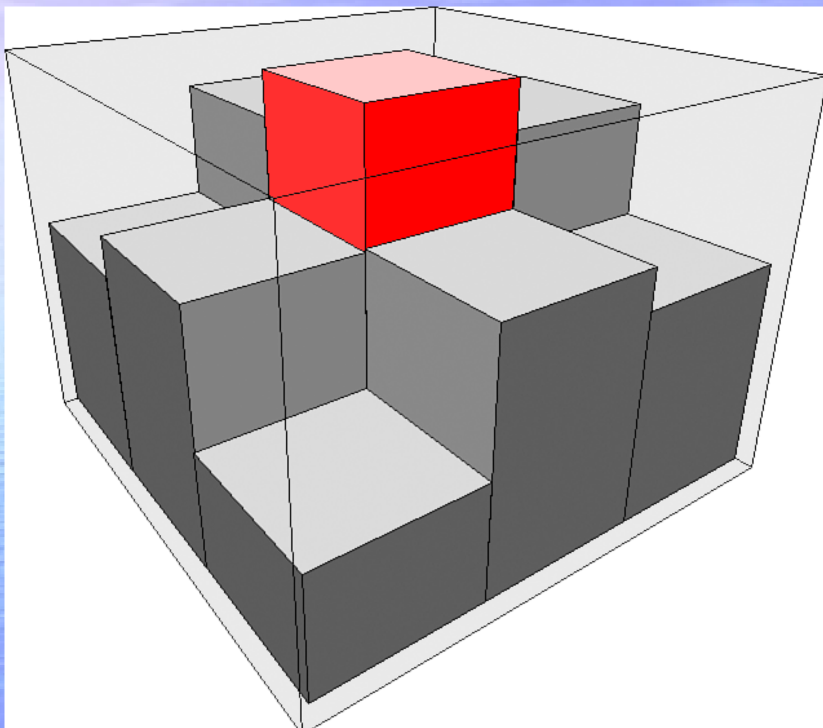

Local maximum of the
normalized point weight

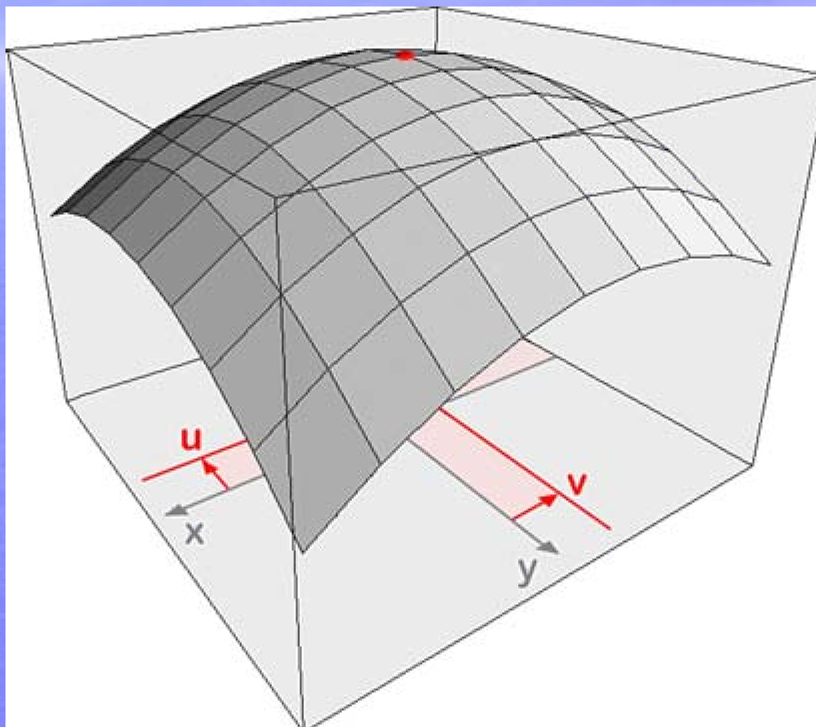


Adapted surface
of the paraboloid

# Paraboloid Fitting

- Paraboloid Function: $w(x,y) = ax^2 + by^2 + cxy + dx + ey + f$

$$\mathbf{A} = \begin{bmatrix} 1 & 1 & 1 & -1 & -1 & 1 \\ 0 & 1 & 0 & 0 & -1 & 1 \\ 1 & 1 & -1 & 1 & -1 & 1 \\ 1 & 0 & 0 & -1 & 0 & 1 \\ 0 & 0 & 0 & 0 & 0 & 1 \\ 1 & 0 & 0 & 1 & 0 & 1 \\ 1 & 1 & -1 & -1 & 1 & 1 \\ 0 & 1 & 0 & 0 & 1 & 1 \\ 1 & 1 & 1 & 1 & 1 & 1 \end{bmatrix}$$

$$\begin{bmatrix} a \\ b \\ \vdots \\ f \end{bmatrix} = \left(\mathbf{A}^{\mathrm{T}}\mathbf{A}\right)^{+} \mathbf{A}^{\mathrm{T}} \begin{bmatrix} w_1 \\ w_2 \\ \vdots \\ w_9 \end{bmatrix}$$

- Sub-Pixel Offset $(x+u, y+v)$:

$$u = \frac{(2bd - ce)}{(c^2 - 4ab)} \qquad v = \frac{(2ae - cd)}{(c^2 - 4ab)}$$

# Sub-Pixel Test Pattern

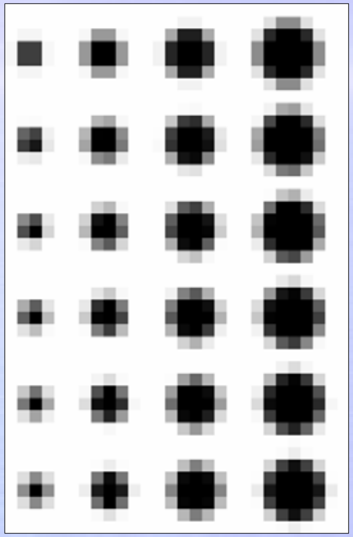

a) Without Noise

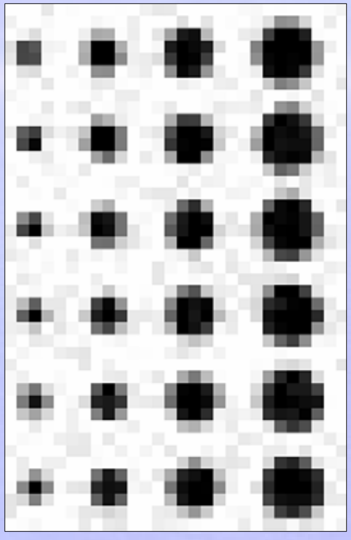

b) 10% Noise

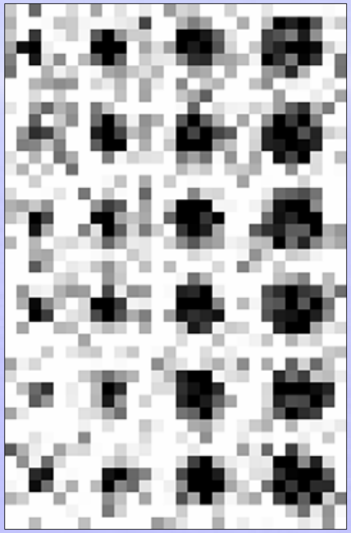

c) 25% Noise

| Noise [%] | Mean error [pixel] | | | | Maximum error [pixel] | | | | Resolution [pixel] | Reliability [pixel] |
|---|---|---|---|---|---|---|---|---|---|---|
| | 2 | 3 | 4 | 5 | 2 | 3 | 4 | 5 | | |
| **0** | 0.029 | 0.030 | 0.024 | 0.023 | 0.052 | 0.045 | 0.045 | 0.059 | **1 / 37** | **1 / 19** |
| **10** | 0.058 | 0.038 | 0.043 | 0.037 | 0.116 | 0.104 | 0.115 | 0.175 | **1 / 22** | **1 / 7** |
| **25** | 0.147 | 0.148 | 0.116 | 0.135 | 0.462 | 0.668 | 0.424 | 0.481 | **1 / 7** | **1 / 2** |

# Extension for Color Images

Autocorrelation Matrix for RGB color images (MONTESINOS, 1998) :

$$\mathbf{A}_{RGB}(x,y)=\begin{bmatrix}\sum\left(r_x^2+g_x^2+b_x^2\right) & \sum\left(r_xr_y+g_xg_y+b_xb_y\right)\\ \sum\left(r_xr_y+g_xg_y+b_xb_y\right) & \sum\left(r_y^2+g_y^2+b_y^2\right)\end{bmatrix}$$

Test Pattern :

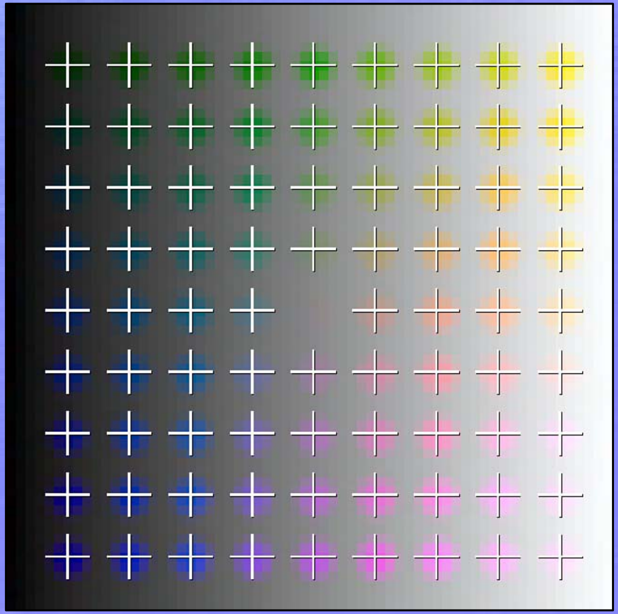

# Optimized Point Distribution

a) Global Threshold

b) Dynamic Threshold

# Detection in Ideal Images

- Reference Image of Smith & Brady (1997)

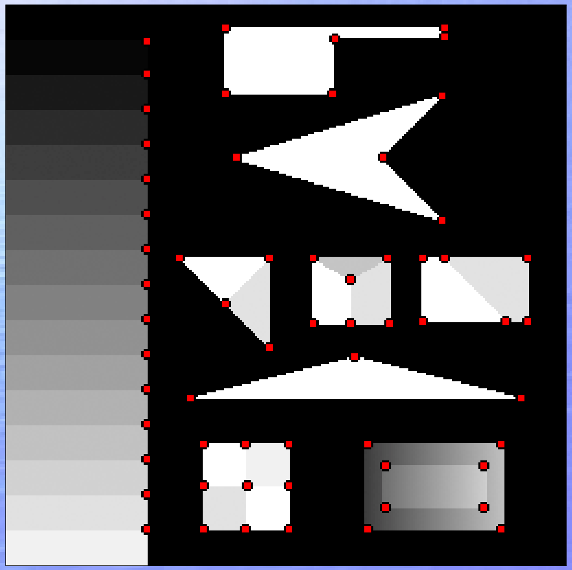

SUSAN-2D Operator

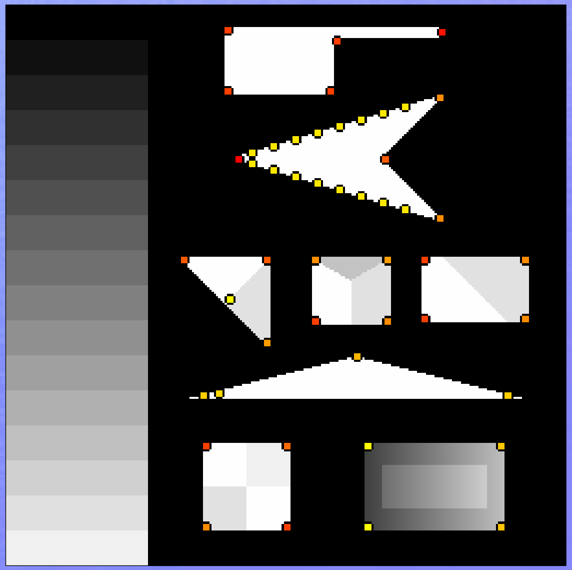

Plessey Point Detector

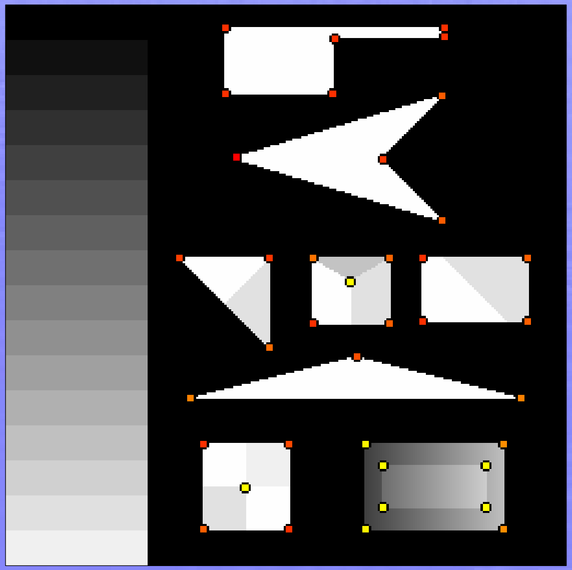

Förstner Operator

# Detection in Synthetic Images

- Reference Image of Rosenthaler (1992)

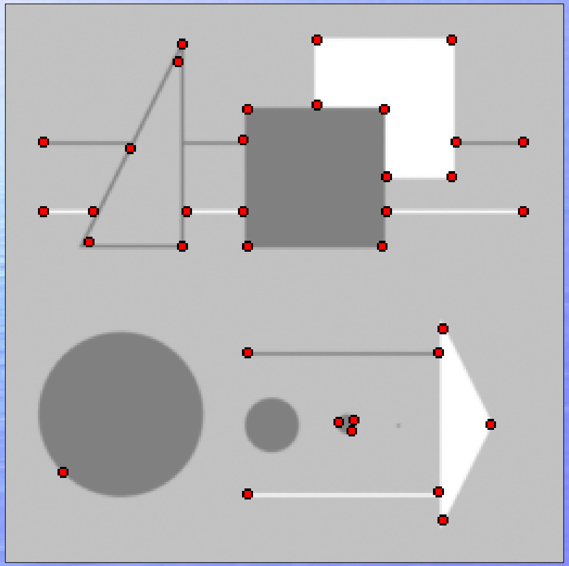

**SUSAN-2D Operator**

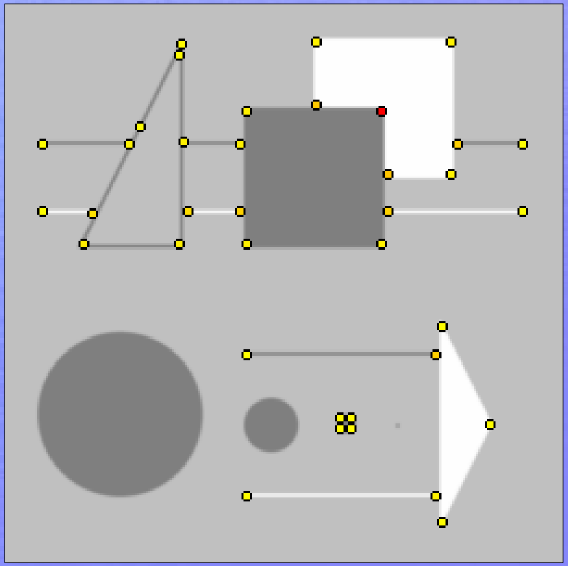

**Plessey Point Detector**

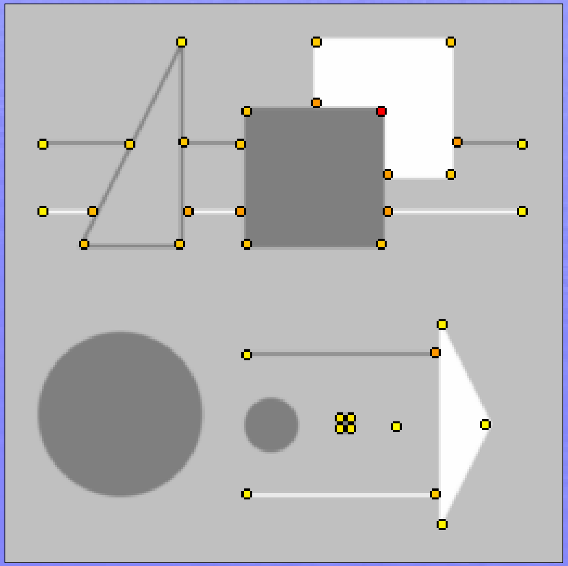

**Förstner Operator**

# Transformed Test Pattern

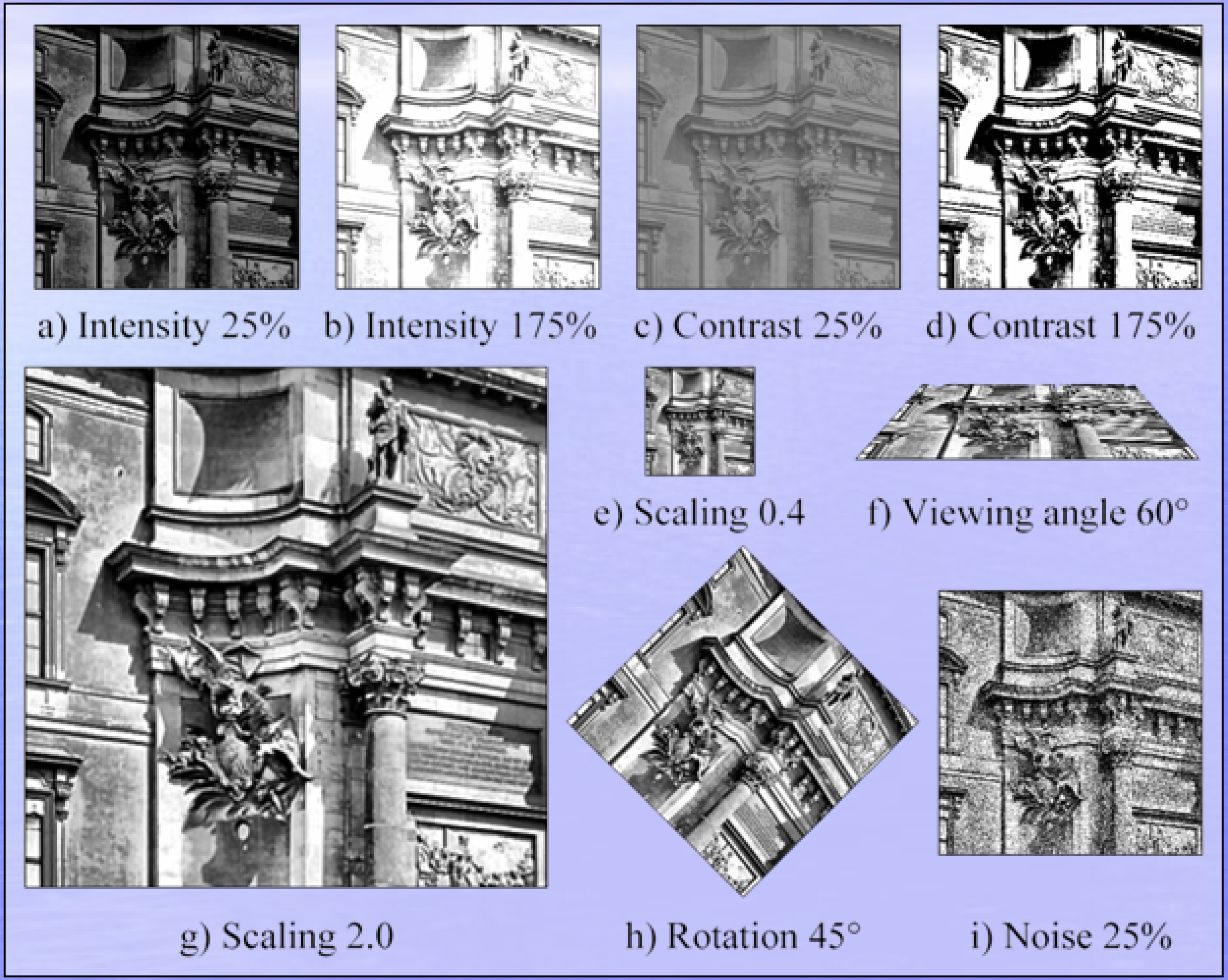

# Repeatability Rates

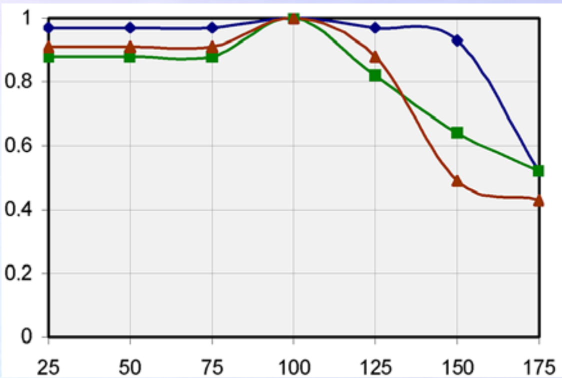

a) Relative Intensity [%]

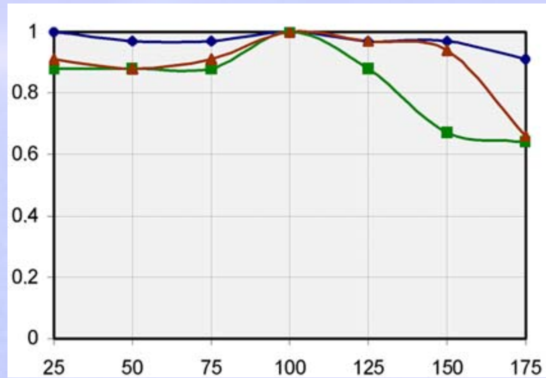

b) Relative Contrast [%]

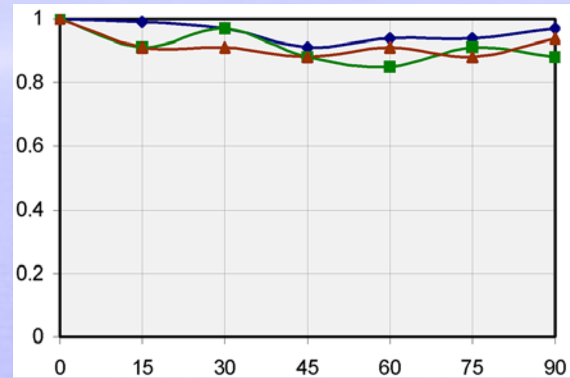

c) Rotation Angle [deg.]

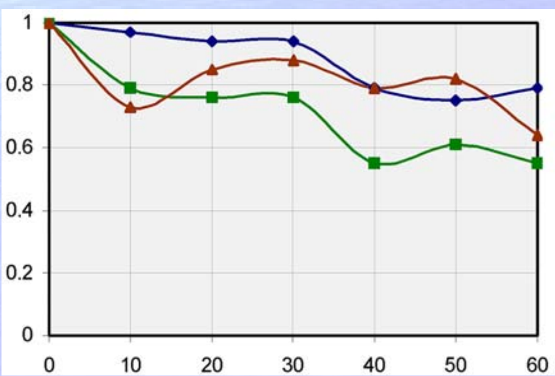

d) Viewing Angle [deg.]

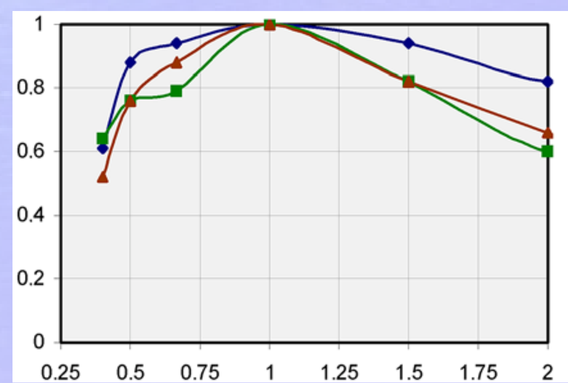

e) Scaling Factor

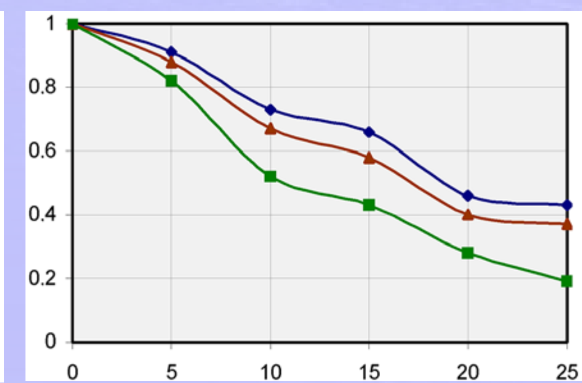

f) Noise [%]

**Method:** Susan-2D ■, Plessey ▲ and Förstner ◆

# Evaluation Summary

| Detector | Detection rate | | Repeatability rate | | | | | | Locali-zation |
|---|---|---|---|---|---|---|---|---|---|
| | Smith | Rosen. | Inten. | Contr. | Rot. | View | Scale | Noise | |
| **SUSAN-2D** | 160* | 78 | 80 | 83 | 92 | 72 | 74 | 54 | 0.34 |
| **Plessey** | 24 | 86 | 79 | 90 | 92 | 82 | 74 | 65 | 0.29 |
| **Förstner** | 100 | 100 | 90 | 97 | 96 | 88 | 86 | 70 | 0.28 |

*** Resulting from edge features**

# INRIA Reference Image

**Valbonne Church, France**

# Conclusions and Outlook

- Interest Operator supply **stable point features** for image matching and object tracking
- Contrary to (Schmid et al., 2000) the **Förstner operator** obtained the best results
- For a comparison, the **implementation** is of major importance
- **Recommendations**
  - Use of **continuous differential operators**
  - Sub-Pixel localization for isolated points with **paraboloid fitting**
  - Extension for **color images**
  - Optimization of the point distribution with a **dynamic threshold**

# Remaining Challenges

- Systematic Localization Error: